Nitrous Oxide detection at 5.26 μm with a compound glass Antiresonant Hollow-Core Optical Fiber

PIOTR JAWORSKI,[1,*] KAROL KRZEMPEK,[1] GRZEGORZ DUDZIK,[1] PIER J. SAZIO,[2] AND WALTER BELARDI[3]

[1]*Laser & Fiber Electronics Group, Faculty of Electronics, Wroclaw University of Science and Technology, 50-370 Wroclaw, Poland*
[2]*Optoelectronics Research Centre, University of Southampton, Highfield, Southampton, Hampshire SO17 1BJ, UK*
[3]*Université de Lille, CNRS, UMR 8523—PhLAM—Physique des Lasers, Atomes et Molécules, F-59000 Lille, France*
**Corresponding author: piotr.jaworski@pwr.edu.pl*

Received XX Month XXXX; revised XX Month, XXXX; accepted XX Month XXXX; posted XX Month XXXX (Doc. ID XXXXX); published XX Month XXXX

Laser-based gas sensors utilizing various light-gas interaction phenomena have proved their capacity for detecting different gases. However, achieving reasonable sensitivity, especially in the mid-Infrared, is crucial. Improving sensors detectivity usually requires incorporating multipass cells, which increase the light-gas interaction path-length at a cost of reduced stability. An unconventional solution comes with the aid of hollow-core fibers. In such fiber light is guided inside an air-core, which when filled with the analyte gas can serve as a low-volume and robust absorption cell. Here, we report on the use of a borosilicate Antiresonant Hollow-Core Fiber for laser-based gas sensing. Due to its unique structure and guidance, this fiber provides low-loss, single-mode transmission >5 μm. The feasibility of using the fiber as a gas cell was verified by detecting NO at 5.26 μm with a minimum detection limit of 20 ppbv. © 2019 Optical Society of America

http://dx.doi.org/10.1364/AO.99.099999

Since its first demonstration in 1999 [1], hollow-core fiber (HC) technology has attracted significant attention throughout the scientific community. Researchers working on this type of waveguide strive to develop novel fiber designs capable of low-loss guidance of light within spectral ranges spanning from the ultraviolet (UV) up to mid-Infrared (mid-IR) [1-8]. Due to the unique ability to guide light with low-loss in an air-core, such fibers overcome limitations connected with high dispersion, damage threshold, nonlinear effects and maximum operating wavelength range, that restrict the use of conventional solid core silica fibers. Hence, HCs paved the way for a broad range of new applications for glass-based fibers. The last decade has shown that HCs can be successfully implemented in e.g. delivery of high power pulsed laser light [9-11], pulse compression [12,13], supercontinuum generation [14], optical imaging [15], and as a novel gain media for gas-based lasers [16-18]. Another very interesting application of HCs is laser-based gas sensing. The hollow core of such fibers can be relatively easily filled with any gas analyte, thus forming a low-volume gas cell. The length of the HC fiber can be tailored to a desired value, serving as an alternative solution to commonly used multipass cells, that optically increase light-gas molecules interaction length, leading to a significant enhancement of the sensor detection performance [19,20]. Multipass cells, however, are usually bulky, fragile, expensive and foremost sensitive to environmental noise and temperature drifts thus increasing the complexity of the sensing system and limiting the application area. Hence, a less complex and more versatile solution, e.g. based on an HC-based low-volume gas absorption cell is desirable. Currently, several types of HCs have been successfully used in laser-based gas sensing. In [21-23] a photonic-bandgap hollow-core photonic crystal fiber (HCPCF) was investigated, proving its capability for sensing various gas molecules in the 1.5 μm and 3.1 μm wavelength region. Unfortunately, implementing HCPCFs as a part of gas sensors is limited by their highly multimode nature, which leads to intermodal interferences, rapidly decreasing the sensor detection performance. Therefore, achieving satisfactory detection limit in a sensor using this particular kind of fiber, usually requires combining it with sophisticated spectroscopic techniques e.g. Chirped Laser Dispersion Spectroscopy (CLaDS) or photothermal spectroscopy [24,25]. Another limitation arises from small core sizes of the HCPFs resulting in a very long gas exchange time, significantly reducing the responsivity of the sensor [24]. Furthermore, due to optical guidance limitations of the HCPCFs it is impossible to use them for efficient trace gas detection in the mid-IR spectral range. A Kagome type HC fiber has been recently demonstrated to overcome majority of the limitations that are present in photonic bandgap fibers. In [26,27] Kagome fibers have been successfully used for gas detection at single ppmv (parts per million by volume) level in the mid-IR. Such fibers have several times bigger core

size and significantly better modal stability in comparison with HCPCFs, which results in a relatively fast gas exchange time (<10 s for ~ 1 m fiber) and less pronounced noise arising from intermodal interference [26]. However, due to their multimode nature, especially evident for longer wavelengths, such fibers are not the perfect candidate for efficient gas sensing. An Antiresonant Hollow Core Fiber (ARHCF) is another type of air-core fiber (with the same guidance mechanism to Kagome fiber, but less complex structure) that has been used for CO_2 sensing at 2 μm, showing better sensor stability than reported using a Kagome fiber [28]. However, the proposed in [28] fiber is also shown to support transmission of higher order modes, that results in the rise of optical fringes in the retrieved spectroscopic signal. It was shown that this issue can be minimized under proper light coupling condition into the ARHCF, however cannot be eliminated (the noise due to intermodal interference is still present in the measured signal), and requires very frequent calibration of the coupling optics between the laser and the fiber. This significantly lowers the robustness and reliability of the reported sensor. As a properly optimized and fabricated ARHCF have the ability to guide light in pure single-transversal-mode regime in both near- and mid-infrared spectral regions they should serve as the perfect choice for gas sensors using optical fibers as low-volume absorption cells. However, implementation of properly designed and fabricated ARHCFs for gas sensing at wavelengths above 5 μm has not been reported yet. In this work, we report the first demonstration of efficient nitrous oxide (NO) sensing inside a compound glass ARHCF at 5.26 μm.

The ARHCF used in the experiments was fabricated from borosilicate glass (DURAN 8330), it was 1.15 m long and consisted of a cladding formed by 8 non-touching circular capillaries and a hollow-air-core with a dia. of 122 μm [29]. A cross-section of the fiber is shown in Fig. 1(a) as an inset. The light guidance mechanism in such fiber structure is realized by the so-called Antiresonant Reflecting Optical Waveguiding mechanism – ARROW [5]. The structural separation between the cladding tubes in the fiber cross section resulted in a very broad and uniform low-loss transmission window [8], and the thin thickness of the cladding tubes (1.4 μm) allowed an anti-resonant band spanning over 1.6 μm in the mid-IR, as can be seen in Fig. 1(a). The fiber exhibits loss at the level of ~4 dB/m above 5 μm wavelength and single-mode behavior, which is desired in fiber-based spectroscopy systems. More details about the fiber can be found in ref. [29].

The experimental setup is shown in Fig. 2. A narrow-linewidth Distributed Feedback Quantum Cascade Laser (DFB-QCL, Thorlabs QD5500CM1) was used as a NO molecules excitation source. The laser was connected to a Thorlabs ITC4002QCL current and temperature driver, which controlled its operation parameters.

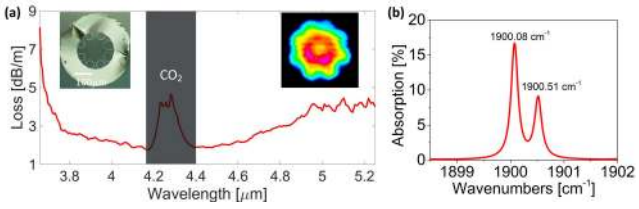

Fig. 1. (a) Attenuation spectrum of the ARHCF showing its performance in the first anti-resonant transmission band. Increase in loss visible around 4.3 μm is due to the presence of atmospheric CO_2 inside the fiber core [29]. A cross-section of the fiber – left; a near-field delivered beam profile at 5.26 μm – right. (b) Hitran simulation of 100 ppmv NO absorption within 1.15 m path length and 900 Torr pressure [30].

The set point current and temperature was fixed at 290 mA and 23.03 °C, respectively, in order to tune the QCL emission to the center of the selected NO transition located at ~5.26 μm (1900.08 cm^{-1}), shown in Fig. 1(b). An arbitrary function generator (FG, Tektronix AFG3102C) was used to apply a sinusoidal modulation (at frequency f_0) and a low-frequency ramp signal to the laser current by driving the modulation input of the laser controller. The QCL output beam was collimated using a Black diamond aspheric lens with a NA of 0.56 and a focal length of 5.95 mm (Edmund Optics 87-178) providing 5 mm dia. beam, which was subsequently focused onto the fiber core using a plano-convex calcium fluoride (CaF_2) lens with a focal length of 75 mm, forming a focus cone angle of ~ 0.066 rad matching the NA of the fibers core mode [8]. Optimized coupling conditions resulted in excitation of the fundamental mode. The other end-facet of the ARHCF was glued-in into a custom-3D-printed airtight housing (gas filling cell) including a light out-coupling aperture sealed with a barium fluoride (BaF_2) wedge (Thorlabs WW01050-E1) and a ¼" gas port supporting efficient gas filling from one end of the fiber. The beam exiting the fiber was focused with a plano-convex CaF_2 lens (f = 50 mm) onto a mercury-cadmium-telluride (MCT) photodetector (VIGO PVI-4TE-8/VPAC-1000F). Signal from the photodetector was forwarded to a lock-in amplifier (LIA, SRS SR830) along with the reference signal (f_0) from the FG. The LIA was set to detect the second harmonic of the modulation applied to the QCL ($2xf_0$). The retrieved signal was digitized using an acquisition card (NI USB-4432) connected to a PC.

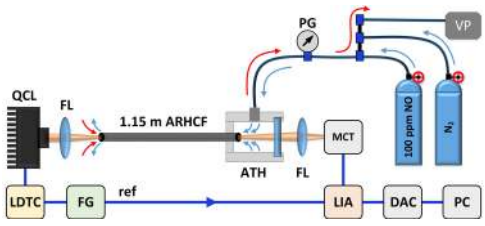

Fig. 2. Experimental setup. QCL – quantum cascade laser, LDTC – laser driver with temp. control, FG – function generator, FL – lenses, ATH – airtight gas filling cell, MCT – photodetector, LIA– lock-in amplifier, DAC – digital acquisition card, PG – pressure gauge, VP – vacuum pump. Electrical cables are in blue, gas tubes are shown as black lines.

The ARHCF used in the experiments was filled with a gas mixture of 100 ppmv NO balanced with nitrogen (N_2) under a controlled and constant overpressure of 900 Torr. Such conditions permitted undisturbed gas flow through the entire length of the fiber. Wavelength Modulation Spectroscopy (WMS) technique was applied to retrieve NO absorption signal of the molecules inside the hollow-core [31]. Parameters optimal for WMS detection at the second harmonic of the modulation frequency ($2xf_0$) were determined experimentally. As shown in Fig. 3(a) and Fig. 3(b) the optimum wavelength modulation amplitude and frequency of the sinusoidal modulation were found to be ~7.5 GHz and 10 kHz, respectively. An additional ramp signal at a frequency of 200 mHz was added to the laser injection current in order to tune the laser wavelength over the entire selected gas absorption line, thus enabling registering the full 2f WMS signal spectra. The recorded 2f WMS signal spectrum is presented in Fig. 3(c). By reducing the wavelength modulation amplitude to ~ 5.3 GHz and increasing the wavelength sweep range it was possible to clearly observe both NO transitions from the doublet present in the considered wavelength regime. Please note that the decrease in the ratio between the absorption line amplitudes in comparison with the HITRAN simulation shown in Fig. 1(b) is caused by the different optical power at which

both transitions were recorded. As the laser wavelength was tuned by changing the laser injection current (via ramp signal), the optical power also varied. Since the amplitude of 2f WMS signal depends on the optical signal level, the lack of correlation between simulation and measurement result is visible. It can be evidently seen that the retrieved WMS signals are smooth and unaffected by the presence of strong optical fringes, which confirms pure single-mode guidance of the fiber and lack of higher-order modes that especially manifest themselves during wavelength tuning and modulation of the QCL. The additional peaks visible at ~ 1899.6 cm^{-1} and 1900.7 cm^{-1} in Fig. 3(d) are connected with the start and end points of the ramp signal, resulting in rapid switching between high and low injection current levels applied to the QCL. Furthermore, to confirm single-mode nature of the ARHCF the out-coupled beam was characterized by directly imaging its end facet onto a DataRay WinCamD beam profiler. The captured near-field delivered beam profile depicted in Fig. 1(a) confirms guidance in the LP01 mode.

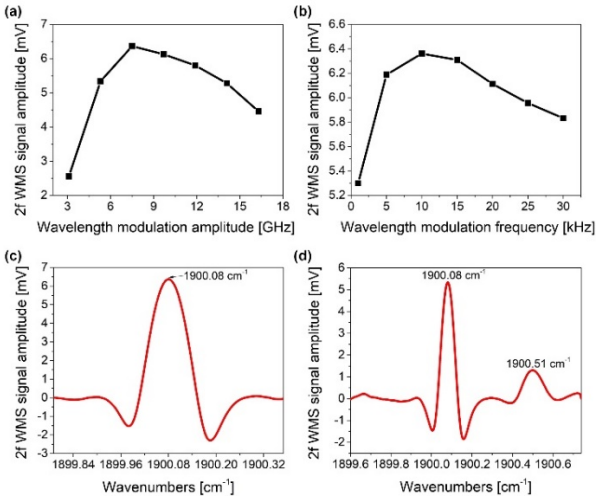

Fig. 3. (a) 2f WMS signal amplitude vs. QCL wavelength modulation amplitude. (b) 2f WMS signal amplitude vs. QCL wavelength modulation freq. (c) Retrieved 2f WMS signal at optimum modulation parameters registered for 100 ppmv NO inside the 1.15 m ARHCF. (d) 2f WMS spectra from two NO transitions obtained with ~5.3 GHz modulation depth in the 1.15 m ARHCF filled with 100 ppmv NO.

The response time of the ARHCF-based gas sensor was estimated by measuring gas exchange time inside the fiber core. The QCL wavelength was actively locked at the center of the selected NO transition (using a PID controller-based feedback loop) and the fiber was firstly flushed with pure nitrogen (with 900 Torr overpressure) in order to fully empty the core and register the baseline signal. After ~4 s we began to fill the fiber with a mixture of 100 ppmv NO balanced with N_2 with 900 Torr overpressure. As shown in Fig. 4, the 2f WMS signal reached its 90% amplitude after the time period of ~9 s, which means that the fiber core was entirely filled with NO at a flow rate of 90 µl/min. This measurement confirms, that the time required for a complete exchange of the gas inside the 1.15 m-long ARHCF is comparable with the results obtained in gas sensors utilizing Kagome type fiber with similar core size and length, yet is more than two orders of magnitude shorter than in conventional HCPCFs [22,24]. The relatively short filling time assures that the ARHCF can be conveniently used as a low-volume gas absorption cell for sensing applications at wavelengths significantly longer than previously reported.

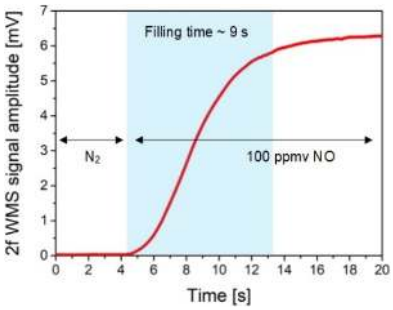

Fig. 4. Gas exchange time measured by registering the 2f WMS signal amplitude change while the fiber was alternately flushed with N_2 and 100 ppmv NO using an overpressure of 900 Torr.

The ARHCF-based NO sensor minimum detection limit (MDL) was estimated by measuring the signal to noise ratio (SNR) and additionally verified by calculating the Allan-Werle deviation. Long-term 2f amplitude noise measurement was performed by stabilizing the QCL wavelength at the center of the gas absorption line at 1900.08 cm^{-1} using a PID-based feedback loop locked at the third harmonic signal from a 10 cm long reference gas cell of filled with 1000 ppmv NO balanced with N_2. The procedure of determining the MDL of the ARHCF-based sensor is based on the work reported in [32]. Firstly, the fiber was filled with 100 ppmv NO in N_2 in order to register the maximum amplitude of the 2f WMS signal, which was equal to 6.34 mV, as shown in Fig. 5 in the range between 0 – 10 s. Next, the ARHCF core was filled with pure N_2 and the data points were collected every 100 ms for a period of 50 min. As can be seen in Fig. 5, the 1σ noise (standard deviation) did not exceed 8.6 µV, yielding a SNR of 737, hence the MDL was ~136 ppbv (parts-per-billion by volume) for SNR equal to unity (for signal integration time of 100 ms). The performance of the sensor at different averaging times was estimated based on the Allan-Werle plot calculated from the data set presented in Fig. 5 (within the time range of 1 – 50 min) [33]. The calculation results plotted in Fig. 6 show that MDL for 1 s and 70 s integration times reached ~30 ppbv and ~20 ppbv, respectively.

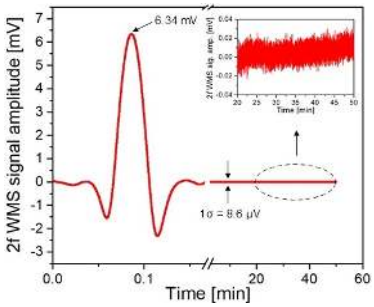

Fig. 5. 2f WMS signal spectrum acquired within single scan of the laser wavelength across NO transition at 1900.08 cm^{-1} together with 2f WMS signal amplitude recorded for a period of 50 min while the ARHCF was flushed with 100 ppmv NO and N_2, respectively.

Based on these measurements the minimum fractional absorption (MFA) was at the level of 2.28×10^{-3}, which is nearly two times better in comparison to results obtained for a sensor based on a Kagome-type HC fiber, targeting methane at 3.4 µm [27]. Furthermore, the obtained MDL is only six times worse in comparison with a sensor utilizing more complex Quartz-enhanced photoacoustic spectroscopy (QEPAS)

method aimed on detection of NO at 1900.08 cm^{-1} [34], showing an excellent potential of ARHCF-based system for efficient gas sensing.

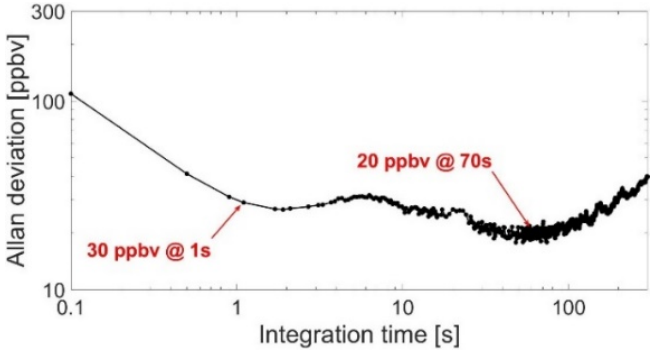

Fig. 6. Allan-Werle plot calculated from the data acquired during 50 min measurement of 2f WMS signal amplitude while the ARHCF was flushed with N_2 and the QCL was actively locked at 1900.08 cm^{-1}.

In this work, to the best of our knowledge, the first demonstration of a gas sensor using a hollow-core fiber as a low-volume absorption cell at a wavelength above 5 μm was presented. Due to excellent transmission characteristic of the fiber and its pure single-mode nature it was possible to obtain a MDL at the level of a few tens of ppbv (20 ppbv at a 70 s signal integration time), which has not been achieved up to date in any hollow-air-core fiber-based gas sensor utilizing WMS technique in this wavelength range. Furthermore, the obtained results are at the level comparable with the performance offered by more complex fiber- or conventional optics-based sensors aided with advanced laser spectroscopy techniques such as photothermal spectroscopy, CLaDS or QEPAS [23,24,34]. The fiber due to its large core size enables relatively fast gas exchange time (<10 s at a 1.15 m length), which compared to other HC fibers [24,26,28] ensures fast response of the sensor built in the proposed configuration. We believe that further improvement in sensing capability can be achieved by directly bonding the fiber end facet to the detector structure, while filling the fiber with target analyte via side-holes manufactured along fiber using a femtosecond-pulsed material processing. Moreover, additional elimination of background noise influencing the sensor performance will be possible by combining the presented fiber with the so-called "fringe-immune" spectroscopic techniques, e.g. CLaDS. The QEPTS (Quartz-tuning-fork enhanced photothermal spectroscopy) method is another interesting approach to increase the sensitivity in ARHCF-based gas sensor [35]. The gas-filled fiber could substitute conventional bulk-optics-based absorption cell used in the reported setup. By carefully focusing the light out-coupled from the fiber onto a quartz-tuning-fork, and subsequently heating up its structure at a strictly defined spot a deviation in the resonance frequency can be observed, which can serve as an alternative method for efficient absorption signal detection. Additionally, further development of the HC structure and basic material may allow similar optical properties at the wavelength range up to 7 μm. An access to an ARHCF operating at this spectral regime will significantly broaden the application area of ARHCF technology in laser-based spectroscopy of gases hazardous for both environment and human life.

Funding. This work was supported by Wroclaw University of Science and Technology (049U/0025/19).

Disclosures. The authors declare no conflicts of interest.

REFERENCES

1. R. F. Cregan, B. J. Mangan, J. C. Knight, T. A. Birks, P. St. J. Russell, P. J. Roberts, and D. C. Allan, Science **285**, 1537 (1999).
2. P. J. St Russell, Science **299**, 358 (2003).
3. F. Couny, F. Benabid, and P. S. Light, Opt. Lett. **31**, 3574 (2006).
4. J. C. Knight, T. A. Birks, P. St. J. Russell, D. M. Atkin, Opt. Lett. **21**, 1547 (1996).
5. N. M. Litchinitser, A. K. Abeeluck, C. Headley, B. J. Eggleton, Opt. Lett. **27**, 1592 (2002).
6. F. Yu and J. C. Knight, IEEE J. Sel. Top. Quant. **22**, 4400610 (2016).
7. I. A. Bufetov, A. F. Kosolapov, A. D. Pryamikov, A. V. Gladyshev, A. N. Kolyadin, A. A. Krylov, Y. P. Yatsenko, and A. S. Biriukov, Fibers **6**, 39 (2018).
8. W. Belardi and J. C. Knight, Opt. Letters **39**, 1853 (2014).
9. P. Jaworski, F. Yu, R. M. Carter, J. C. Knight, J. D. Shephard, and D. P. Hand, Opt. Express **23**, 8498 (2015).
10. P. Jaworski, F. Yu, R. R. J. Maier, W. J. Wadsworth, J. C. Knight, J. D. Shephard, and D. P. Hand, Opt. Express **21**, 22742 (2013).
11. B. Debord, M. Alharbi, L. Vincetti, A. Husakou, C. Fourcade-Dutin, C. Hoenninger, E. Mottay, F. Gérôme, and F. Benabid, Opt. Express **22**, 10735 (2014).
12. K. Murari, G. J. Stein, H. Cankaya, B. Debord, F. Gérôme, G. Cirmi, O. D. Mücke, P. Li, A. Ruehl, I. Hartl, K.-H. Hong, F. Benabid, and F. X. Kärtner, Optica **3**, 816 (2016).
13. T. Balciunas, C. Fourcade-Dutin, G. Fan, T. Witting, A. A. Voronin, A. M. Zheltikov, F. Gerome, G. G. Paulus, A. Baltuska, and F. Benabid, Nat. Commun. **6**, 6117 (2015).
14. L. Chu Van, A. Anuszkiewicz, A. Ramaniuk, R. Kasztelanic, K. Dinh Xuan, V. Cao Long, M. Trippenbach, and. R. Buczyński, J. Opt. **19**, 125604 (2017).
15. M. Andreana, T. Le, W. Drexler, and A. Unterhuber, Opt. Lett. **44**, 1588 (2019).
16. M. Xu, F. Yu, and J. Knight, Opt. Lett. **42**, 4055 (2017).
17. M. R. Abu Hassan, F. Yu, W. J. Wadsworth, and J. C. Knight, Optica **3**, 218 (2016).
18. Y. Cui, W. Huang, Z. Wang, M. Wang, Z. Zhou, Z. Li, S. Gao, Y. Wang, and P. Wang, Optica **6**, 951 (2019).
19. D. R. Herriott and H. J. Schulte, Appl. Opt. **4**, 883 (1965).
20. D. Stachowiak, P. Jaworski, P. Krzaczek, G. Maj, and M. Nikodem, Sensors **18**, 529 (2018).
21. F. Yang, W. Jin, Y. Cao, H. L. Ho, and Y. Wang, Opt. Express **22**, 24894 (2014).
22. A. M. Cubillas, M. Silva-Lopez, J. M. Lazaro, O. M. Conde, M. N. Petrovich, and J. M. Lopez-Higuera, Opt. Express **15**, 17570 (2007).
23. Ł. Kornaszewski, N. Gayraud, J. M. Stone, W. N. MacPherson, A. K. George, J. C. Knight, D. P. Hand, and D. T. Reid, Opt. Express **15**, 11219 (2007).
24. P. Jaworski, Opt. Eng. **58**, 026112 (2019).
25. W. Jin, Y. Cao, F. Yang, H. L. Ho, Nat. Commun. **6**, 6767 (2015).
26. K. Krzempek, K. Abramski, and M. Nikodem, Sensors **19**, 3352 (2019).
27. M. Nikodem, K. Krzempek, G. Dudzik, and K. Abramski, Opt. Express **26**, 21843 (2018).
28. M. Nikodem, G. Gomółka, M. Klimczak, D. Pysz, and R. Buczyński, Opt. Express **27**, 14998 (2019).
29. W. Belardi and P. J. Sazio, Fibers **7**, 73 (2019).
30. Gordon I., Rothman L., Hill C., Kochanov R., Tan Y., Bernath P., Birk M., Boudon V., Campargue A., Chance K., et al., J. Quant. Spectrosc. Radiat. Transf. **203**, 3 (2017).
31. G. B. Rieker, J. B. Jeffries, and R. K. Hanson, Appl. Opt. **48**, 5546 (2009).
32. A. Sampaolo, P. Patimisco, M. Giglio, L. Chieco, G. Scamarcio, F. Tittel, and V. Spagnolo, Opt. Express **24**, 15872 (2016).
33. P. Werle, Appl. Phys. B **102**, 313 (2011).
34. F. K. Tittel, L. Dong, R. Lewicki, V. Spagnolo, and Y. Zhang, in 2012 Symposium on Photonics and Optoelectronics (IEEE 2012), pp. 1.
35. Y. Ma, Y. He, Y. Tong, X. Yu, and F. K. Tittel, Opt. Express **26**, 32103 (2018).

REFERENCES

1. R. F. Cregan, B. J. Mangan, J. C. Knight, T. A. Birks, P. St. J. Russell, P. J. Roberts, and D. C. Allan, "Single-Mode Photonic Guidance of Light in Air," Science **285**, 1537 (1999).
2. P. J. St Russell, "Photonic Crystal Fibers," Science **299**, 358 (2003).
3. F. Couny, F. Benabid, and P. S. Light, "Large pitch kagome-structure hollow-core photonic crystal fiber," Opt. Lett. **31**, 3574 (2006).
4. J. C. Knight, T. A. Birks, P. St. J. Russell, D. M. Atkin, "All-silica single-mode optical fiber with photonic crystal cladding," Opt. Lett. **21**, 1547 (1996).
5. N. M. Litchinitser, A. K. Abeeluck, C. Headley, B. J. Eggleton, "Antiresonant reflecting photonic crystal optical waveguides," Opt. Lett. **27**, 1592 (2002).
6. F. Yu and J. C. Knight, "Negative Curvature Hollow-Core Optical Fiber," IEEE J. Sel. Top. Quant. **22**, 4400610 (2016).
7. I. A. Bufetov, A. F. Kosolapov, A. D. Pryamikov, A. V. Gladyshev, A. N. Kolyadin, A. A. Krylov, Y. P. Yatsenko, and A. S. Biriukov, "Revolver Hollow Core Optical Fibers," Fibers **6**, 39 (2018).
8. W. Belardi and J. C. Knight, "Hollow antiresonant fibers with reduced attenuation," Opt. Letters **39**, 1853 (2014).
9. P. Jaworski, F. Yu, R. M. Carter, J. C. Knight, J. D. Shephard, and D. P. Hand, "High energy green nanosecond and picosecond pulse delivery through a negative curvature fiber for precision micro-machining," Opt. Express **23**, 8498 (2015).
10. P. Jaworski, F. Yu, R. R. J. Maier, W. J. Wadsworth, J. C. Knight, J. D. Shephard, and D. P. Hand, "Picosecond and nanosecond pulse delivery through a hollow-core Negative Curvature Fiber for micro-machining applications," Opt. Express **21**, 22742 (2013).
11. B. Debord, M. Alharbi, L. Vincetti, A. Husakou, C. Fourcade-Dutin, C. Hoenninger, E. Mottay, F. Gérôme, and F. Benabid, "Multi-meter fiber-delivery and pulse self-compression of milli-Joule femtosecond laser and fiber-aided laser-micromachining," Opt. Express **22**, 10735 (2014).
12. K. Murari, G. J. Stein, H. Cankaya, B. Debord, F. Gérôme, G. Cirmi, O. D. Mücke, P. Li, A. Ruehl, I. Hartl, K.-H. Hong, F. Benabid, and F. X. Kärtner, "Kagome-fiber-based pulse compression of mid-infrared picosecond pulsed from a Ho:YLF amplifier," Optica **3**, 816 (2016).
13. T. Balciunas, C. Fourcade-Dutin, G. Fan, T. Witting, A. A. Voronin, A. M. Zheltikov, F. Gerome, G. G. Paulus, A. Baltuska, and F. Benabid, "A strong-field driver in the single-cycle regime based on self-compression in a kagome fibre," Nat. Commun. **6**, 6117 (2015).
14. L. Chu Van, A. Anuszkiewicz, A. Ramaniuk, R. Kasztelanic, K. Dinh Xuan, V. Cao Long, M. Trippenbach, and. R. Buczyński, "Supercontinuum generation in photonic crystal fibres core filled with toluene," J. Opt. **19**, 125604 (2017).
15. M. Andreana, T. Le, W. Drexler, and A. Unterhuber, "Ultrashort pulse Kagome hollow-core photonic crystal fiber delivery for nonlinear optical imaging," Opt. Lett. **44**, 1588 (2019).
16. M. Xu, F. Yu, and J. Knight, "Mid-infrared 1 W hollow-core fiber gas laser source," Opt. Lett. **42**, 4055 (2017).
17. M. R. Abu Hassan, F. Yu, W. J. Wadsworth, and J. C. Knight, "Cavity-based mid-IR fiber gas laser pumped by a diode laser," Optica **3**, 218 (2016).
18. Y. Cui, W. Huang, Z. Wang, M. Wang, Z. Zhou, Z. Li, S. Gao, Y. Wang, and P. Wang,"4.3 μm fiber laser in CO_2-filled hollow-core silica fibers," Optica **6**, 951 (2019).
19. D. R. Herriott and H. J. Schulte, "Folded Optical Delay Lines," Appl. Opt. **4**, 883 (1965).
20. D. Stachowiak, P. Jaworski, P. Krzaczek, G. Maj, and M. Nikodem, "Laser-Based Monitoring of CH_4, CO_2, NH_3 and H_2S in Animal Farming – System Characterization and Initial Demonstration," Sensors **18**, 529 (2018).
21. F. Yang, W. Jin, Y. Cao, H. L. Ho, and Y. Wang, "Towards high sensitivity gas detection with hollow-core photonic bandgap fibers," Opt. Express **22**, 24894 (2014).
22. A. M. Cubillas, M. Silva-Lopez, J. M. Lazaro, O. M. Conde, M. N. Petrovich, and J. M. Lopez-Higuera, "Methane detection at 1670-nm band using a hollow-core photonic bandgap fiber and a multiline algorithm," Opt. Express **15**, 17570 (2007).
23. Ł. Kornaszewski, N. Gayraud, J. M. Stone, W. N. MacPherson, A. K. George, J. C. Knight, D. P. Hand, and D. T. Reid, "Mid-infrared methane detection in a photonic bandgap fiber using a broadband optical parametric oscillator," Opt. Express **15**, 11219 (2007).
24. P. Jaworski, "Molecular dispersion spectroscopy in a CO_2-filled all-fiber gas cells based on a hollow-core photonic crystal fiber," Opt. Eng. **58**, 026112 (2019).
25. W. Jin, Y. Cao, F. Yang, H. L. Ho, "Ultra-senstivie all-fiber photothermal spectroscopy with large dynamic range," Nat. Commun. **6**, 6767 (2015).
26. K. Krzempek, K. Abramski, and M. Nikodem, "Kagome Hollow Core Fiber-Based Mid-Infrared Dispersion Spectroscopy of Methane at Sub-ppm Levels," Sensors **19**, 3352 (2019).
27. M. Nikodem, K. Krzempek, G. Dudzik, and K. Abramski, "Hollow core fiber-assisted absorption spectroscopy of methane at 3.4 μm," Opt. Express **26**, 21843 (2018).
28. M. Nikodem, G. Gomółka, M. Klimczak, D. Pysz, and R. Buczyński, "Laser absorption spectroscopy at 2 μm inside revolver-type anti-resonant hollow core fiber," Opt. Express **27**, 14998 (2019).
29. W. Belardi and P. J. Sazio, "Borosilicate Based Hollow-Core Optical Fibers," Fibers **7**, 73 (2019).
30. Gordon I., Rothman L., Hill C., Kochanov R., Tan Y., Bernath P., Birk M., Boudon V., Campargue A., Chance K., et al., "The HITRAN2016 molecular spectroscopic databse," J. Quant. Spectrosc. Radiat. Transf. **203**, 3 (2017).
31. G. B. Rieker, J. B. Jeffries, and R. K. Hanson, "Calibration-free wavelength-modulation spectroscopy for measurement of gas temperature and concentration in harsh environments," Appl. Opt. **48**, 5546 (2009).
32. A. Sampaolo, P. Patimisco, M. Giglio, L. Chieco, G. Scamarcio, F. Tittel, and V. Spagnolo, "Highly sensitive gas leak detector based on a quartz-enhanced photoacoustic SF6 sensor," Opt. Express **24**, 15872 (2016).
33. P. Werle, "Accuracy and precision of laser spectrometers for trace gas sensing in the presence of optical fringes and atmospheric turbulence," Appl. Phys. B **102**, 313 (2011).
34. F. K. Tittel, L. Dong, R. Lewicki, V. Spagnolo, and Y. Zhang, "Sensitive Detection of Nitric Oxide Using a Quantum Cascade Laser Based QEPAS Sensor," in 2012 Symposium on Photonics and Optoelectronics (IEEE 2012), pp. 1.
35. Y. Ma, Y. He, Y. Tong, X. Yu, and F. K. Tittel, "Quartz-tuning-fork enhanced photothermal spectroscopy for ultra-high sensitive trace gas detection," Opt. Express **26**, 32103 (2018).